The Third International Bridge Seismic Workshop, 3rd IBSW
Seattle, Washington, USA - October 1st to 4th, 2019

SEISMIC ASSESSMENT OF CONCRETE BALANCED-SYSTEM BRIDGES

A. Orgnoni[1], N. Scattarreggia[2], D. Malomo[3], P.M. Calvi[4], M. Moratti[5], G.M. Calvi[6], R. Pinho[7]

[1] *Modelling and Structural Analysis Konsulting (Mosayk Ltd), Pavia, Italy. Email: andrea.orgnoni@mosayk.it*
[2] *University School for Advanced Studies, IUSS Pavia, Italy. Email: nicola.scattarreggia@iusspavia.it*
[3] *Modelling and Structural Analysis Konsulting (Mosayk Ltd), Pavia, Italy. Email: daniele.malomo@mosayk.it*
[4] *University of Washington, Seattle, USA. Email: pmc85@uw.edu*
[5] *Studio Calvi Ltd, Pavia, Italy. Email: matteo.moratti@studiocalvi.eu*
[6] *University School for Advanced Studies, IUSS Pavia, Italy. European Centre for Training and Research in Earthquake Engineering (EUCENTRE), Pavia, Italy. Studio Calvi Ltd, Pavia, Italy. Email: gm.calvi@studiocalvi.eu*
[7] *Department of Civil Engineering and Architecture, University of Pavia, Italy. Modelling and Structural Analysis Konsulting (Mosayk Ltd), Pavia, Italy. Email: rui.pinho@unipv.it*

Abstract

Concrete balanced-system bridges have recently become an object of interest, especially after the collapse of the Polcevera viaduct (Genoa, Italy), also known as "Morandi bridge", occurred on August 2018 due to currently unknown reasons. Given that several other structures of this type have been erected in earthquake-prone areas, this work focuses on the numerical assessment of their dynamic and seismic response, taking the balance system of the Morandi bridge as a reference. First, nonlinear dynamic analyses were performed using triaxial records compatible with the local seismic hazard, also enabling the estimation of the seismic demand on the different bridge components. Then, since shear mechanisms in some of the members appeared to play a critical role in the seismic assessment of the considered bridge system, their capacity is assessed using both seismic code formulae and more advanced numerical procedures, including the Modified Compression Field Theory.

Keywords: cable-stayed bridges; balanced-system; seismic assessment; numerical modeling

1. Introduction

1.1 Concrete balanced-system bridges in the world

The most notable concrete balanced-system bridges were erected in the 60-70's (see Fig. 1 below), mostly in areas exposed to earthquakes. The objective of this work is thus to investigate and assess the seismic behavior of this kind of concrete bridges, not initially designed to sustain seismic horizontal loading. For this purpose, the viaduct over the Polcevera river, which collapsed on August 2018 claiming the lives of 43 victims, has been selected as a case-study, also because of the availability of several original design documentation and construction details.

Fig. 1 – Balanced-system bridges in the world

1.2 Case study: the viaduct over the Polcevera river (Morandi bridge)

The viaduct over the Polcevera river was built between 1963-1966 and opened in September 1967. The first part of the viaduct, called by the designer "minor spans" [1], is made by six V-shaped piers that support the 36 m long simply-supported spans. The second part, denominated "major spans" [1] (Fig.2) is composed of three balanced systems that support the deck, which are 171.9, 171.9 and 145.7 m long. The first of the two, balanced systems 9 and 10, feature:

- A concrete foundation resting on 150 cm diameter piles (not studied herein);
- A pier made of 8 variable-section inclined props that support the deck at a height of 40.33 m over the foundations level;
- An antenna made by two A-shaped variable sections frames that converge at 90.2 m over the foundations level. This system is independent of the deck-pier system; the two systems are connected only through the stays;
- A main deck composed of a 6-web cellular section of variable height (from 4.5m to 1.8m). The webs' thickness varies from 18 to 30 cm. The upper and the lower slabs, 16 cm thick, are respectively 18 and 15 m wide;
- Two main transverse beams that link the deck with the stays and two transverse beams that connect the deck to the pier;
- Four post-compressed concrete stays that connect the upper part of the antenna with the deck, with a slope of about 30°.
- Two 36 m long simply-supported spans made of 6 precast beams of variable height and an upper slab 16 cm thick and 18 m wide. These two systems rest on the Gerber saddles at the end of the main deck. [1][2]

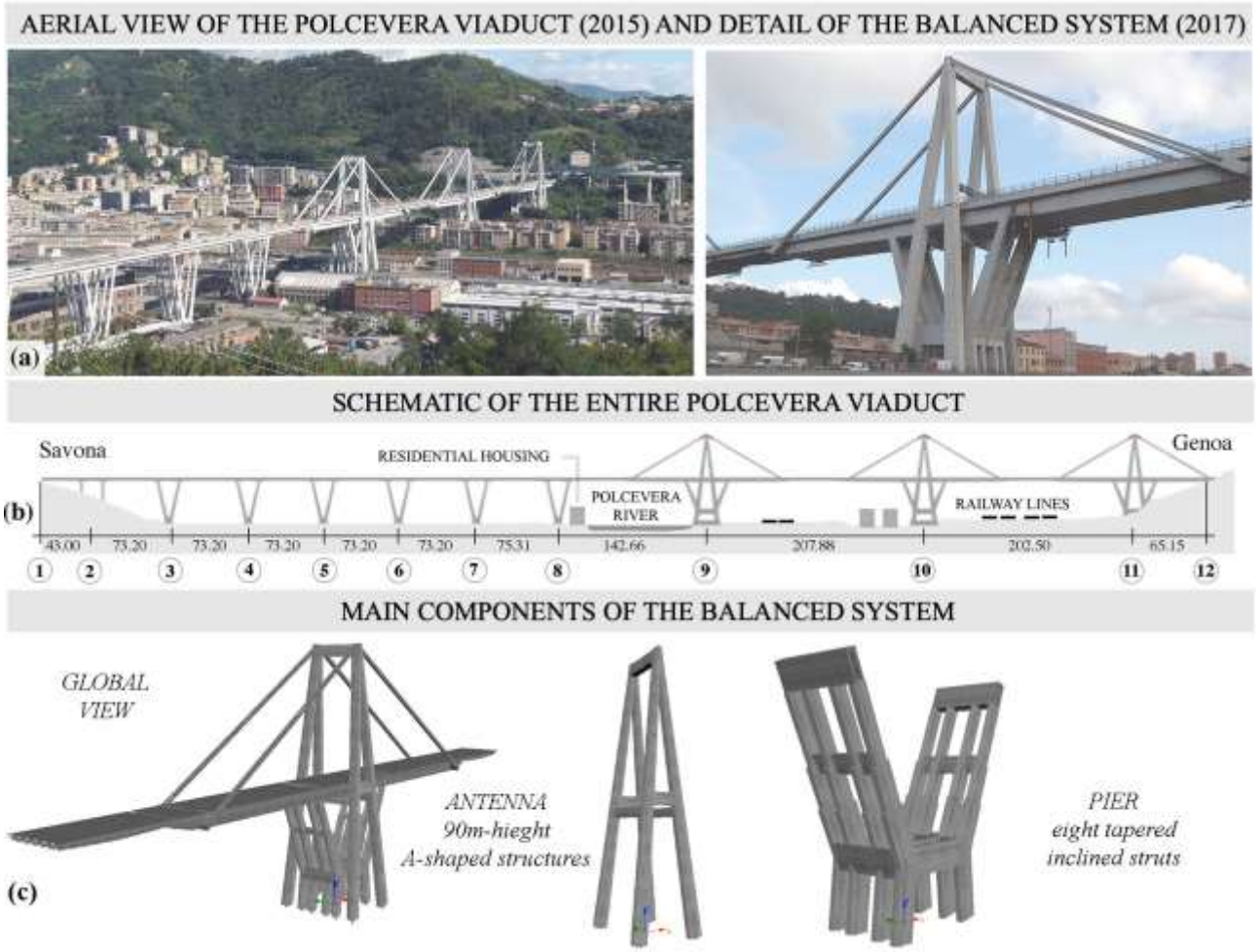

Fig. 2 – (a) Aerial photo of the bridge (left) and of a balanced system (right), (b) viaduct schematization and (c) main components of the balanced system, designed by Morandi [1]

2. Modelling approach and assumptions

The modelling of the collapsed portion of the Polcevera Viaduct has been developed with the software SeismoStruct [3], a well-known finite-element software capable of performing nonlinear inelastic analysis through a fiber discretization approach, and particularly suited and validated for seismic analysis [4].

The numerical model, shown in Fig. 2c, has been assembled through the use of displacement-based beam-column elements, for reasons of numerical stability and speed of the analyses. Material inelasticity, on the other hand, has been introduced through the use of the Mander et al. [5] and Menegotto-Pinto [6] constitutive models for concrete (properties in Table 1) and steel (properties in Table 2), respectively.

Table 1 – Main numerical parameters. concrete material (Mander et al. [1])

Parameter	**Concrete 300/730 (Antenna)**	**Concrete 350/730 (Pier, Deck, Stays)**
Mean compression strength	30.9 MPa	42.3 MPa
Mean tensile strength	0 MPa	0 MPa
Mean elastic modulus	34,300 MPa	39,200 MPa

Table 2 – Steel nonlinear constitutive model parameters (Menegotto-Pinto [7])

Parameter	Aq50 (Antenna, Pier)	FeB44 (Deck, Stays)
Mean elastic modulus	210,000 MPa	210,000 MPa
Mean yielding strength	371 MPa	440 MPa

3. Validation of the model

A cross-validation of the model has been performed through comparisons with the results obtained with a Midas Civil [8] model developed by Orgnoni [9] to study the construction sequence of the bridge (Fig. 3). Clearly, static analysis in SeismoStruct and construction stage analysis in Midas Civil are inherently very different from one another, hence identical results are not necessarily to be expected, as further discussed below.

Fig. 3 – Balanced system number 9: (a) Midas Civil, (b) SeismoStruct

2.1 Overall vertical reactions and deformations

As it can be gathered from the results reported in Table 3, the two modeling strategies lead to relatively similar results; in particular, the total vertical base reactions differ from each other by less than 3%. Due to the impossibility of building the stays step-by-step in SeismoStruct, the difference in vertical displacement between the two models can be significant, but this does not affect the behavior of the complete structure.

Table 3 – Comparison between numerical results obtained with the two selected modelling approaches

Response	Midas Civil	SeismoStruct
Total vertical base reactions	223,408kN	224,215kN
Deck extremities vertical displacement	-1.4 cm	-1.58 cm
Middle stay vertical displacement	-90 cm	-46 cm

2.2 Pier and Antenna internal forces

The Antenna and the Pier are two clear examples of different modeling. The Antenna (Fig 4) has been assembled in the two different software in the same way: with no construction sequences. Instead, the Pier was modelled in Midas Civil by means of a series of construction steps [8]. In Table 4 the Antenna and Pier bending moments are compared, along five control sections.

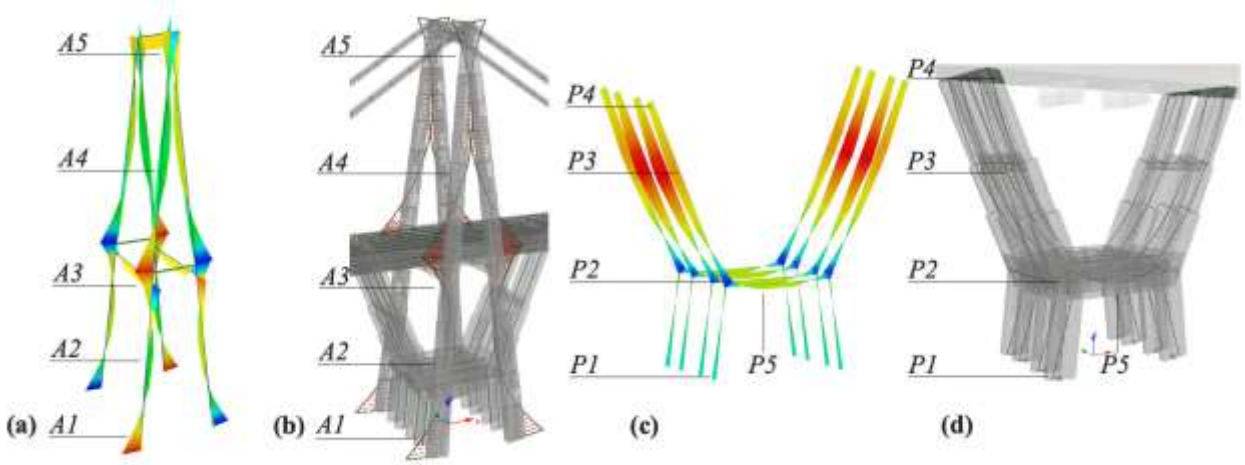

Fig. 4 – (a) Midas Civil Antenna bending moment, (b) SeismoStruct Antenna bending moment, (c) Midas Civil Pier bending moment, (d) SeismoStruct Pier bending moment

Table 4 – Comparison of bending moments obtained with the two selected modelling approaches (in kNm)

Antenna bending moment comparison			**Pier bending moment comparison**		
Sections	**Midas Civil**	**SeismoStruct**	**Sections**	**Midas Civil**	**SeismoStruct**
1	3744.8	-3693.7	1	-1713.2	-2462.8
2	-1226.8	-1244.1	2	-3501.6	-5584.3
3	3681.3	3499.5	3	3718.5	1498.6
4	-1399.9	-1341.4	4	2423.7	-653.4
5	1666.6	1874.8	5	1757.5	1674.1

Concerning the Antenna results, due to the very same modeling of the structure (even if in two different software) they are almost identical. The same cannot be said for the Pier bending moment comparison; Table 4 shows in fact that the internal actions are quite different in the two models (due to the lack of Construction Stage Analysis in SeismoStruct).

2.3 Vibration modes

As depicted in Fig. 5 and summarized in Table 5, the two modeling strategies lead to very comparable eigenvalue solutions. SeismoStruct periods are slightly lower with respect to Midas Civil, probably due to the fact that SeismoStruct considers also the reinforcement stiffness in the sectional stiffness calculation.

Table 5 – Eigenvalues comparisons

RZ fundamental mode		
Software	**Period**	**Participating mass**
Midas Civil	4.66 s	96.8%
SeismoStruct	4.38 s	97.4%
Y fundamental mode		
Software	**Period**	**Participating mass**
Midas Civil	2.28 s	69.8%
SeismoStruct	1.99 s	39.6%
X fundamental mode		
Software	**Period**	**Participating mass**
Midas Civil	1.13 s	62.4%
SeismoStruct	1.04 s	58.6%

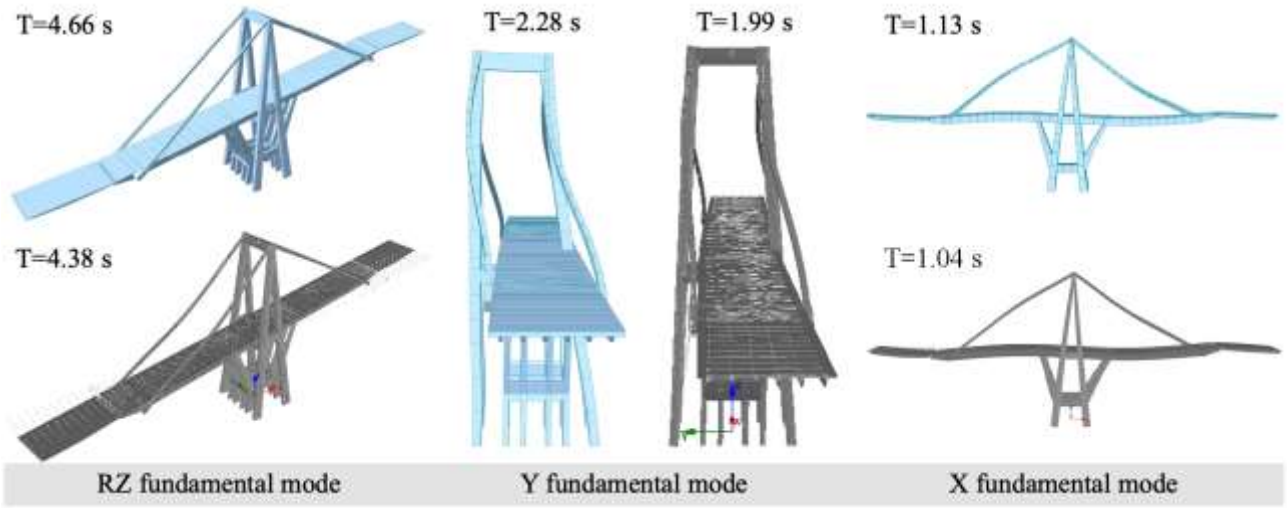

Fig. 5 – Vibration modes comparison

2.4 Nonlinear dynamic response

To compare the nonlinear dynamic behavior of the two models, they have been subjected to an acceleration time-history chosen according to the prescriptions of Italian seismic assessment code (NTC18 [10, 11], see chapter 4), and the displacement time-history responses compared at three different locations:

- Mid-point of the Antenna top transverse beam, to compare the Antenna response (Fig.6);
- Central point of the main deck, to compare the Pier response (Fig.7);
- Extreme point of the main deck, to compare the Deck response (Fig.8).

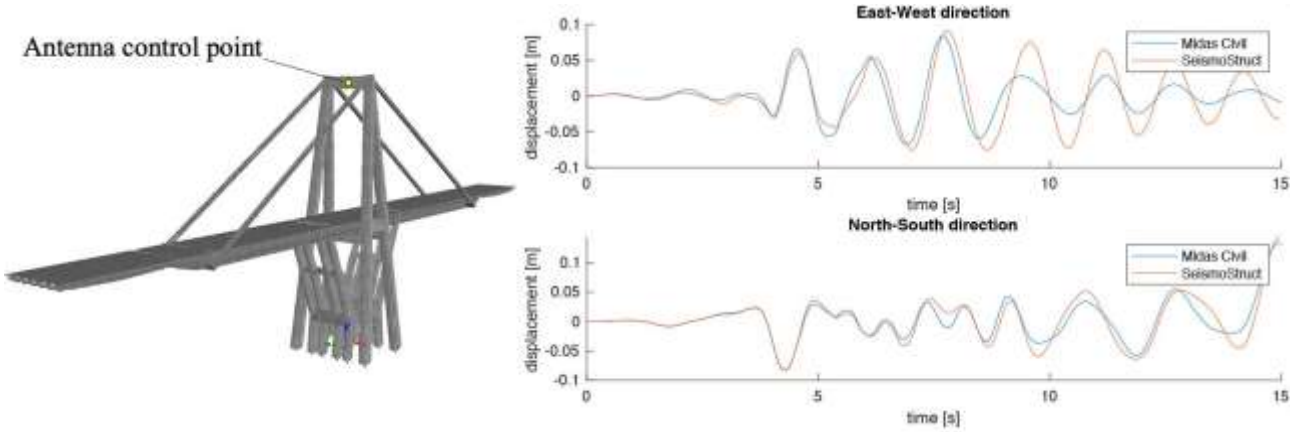

Fig. 6 – Antenna displacements comparison

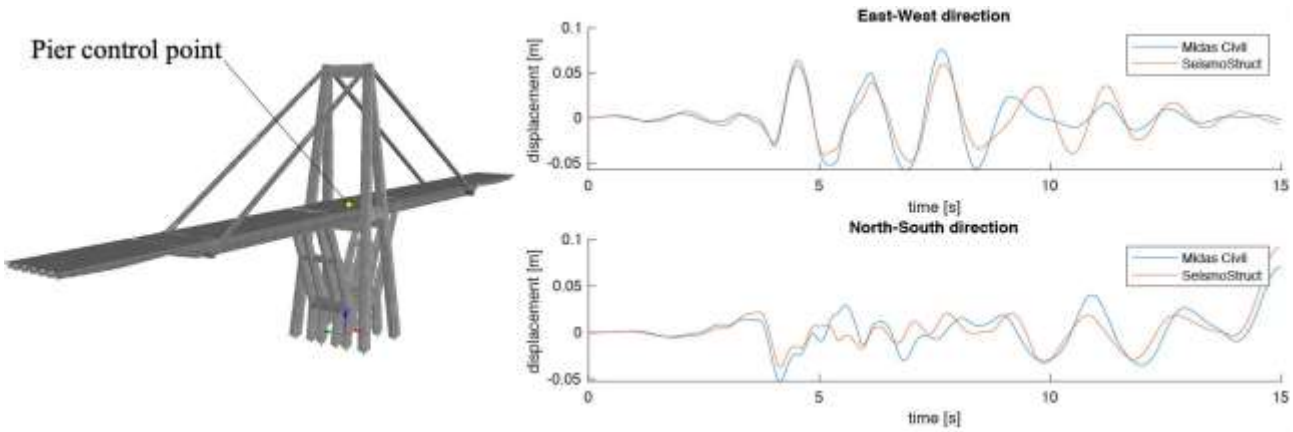

Fig. 7 – Pier displacements comparison

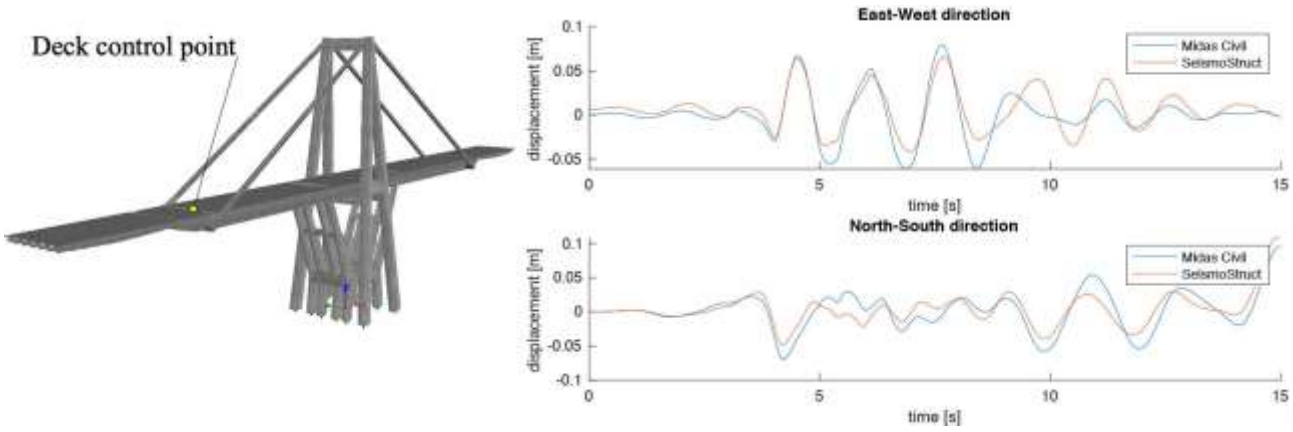

Fig. 8 – Deck displacements comparison

4. Seismic input motion selection

The seismic input motion has been chosen according to the Italian building code NTC18, considering the seismic hazard at the viaduct's geographical coordinates. The parameters characterizing the horizontal and the vertical elastic spectrum, computed for the collapse limit state, are reported in Table 6 and Table 7.

Table 6 – Horizontal elastic spectrum parameters

Limit State	**a_g (g)**	**F_0**	**Tc*(s)**	**S_S**	**C_C**	**S_T**	**q**
Collapse	0.118	2.526	0.306	1.5	1.553	1	1

Table 7 – Vertical elastic spectrum parameters

Limit State	**a_{gv} (g)**	**S_S**	**S_T**	**q**	**T_R (s)**	**T_C (s)**	**T_D (s)**
Collapse	0.055	1	1	1.5	0.05	0.15	1

The natural accelerograms used for the nonlinear dynamic analyses of the bridge, reported in Table 8, have been selected from the ESM database (Engineering Strong Motion Database, http://esm.mi.ingv.it) considering the following parameters: range of Magnitude 4.5-5.5, distance from fault 0-15 km, soil type C, PGA included in the range 0.15-0.3g. The selection of the records has been performed with the software SeismoSelect 2018 [12].

Table 8 – Selected natural signals

Event	Date	Magnitude	EW PGA	NS PGA	Duration
Reggio Emilia	15/10/1996	5.4 Mw	0.27 g	0.18 g	15.0 s
Emilia	25/10/2012	5.2 Mw	0.27 g	0.19 g	15.0 s
Centro Italia	24/08/2016	5.3 Mw	0.20 g	0.23 g	15.0 s
Emilia	29/05/2012	5.5 Mw	0.34 g	0.16 g	20.0 s
Emilia	29/05/2012	5.5 Mw	0.19 g	0.28 g	15.0 s
Irpinia	1/12/1980	4.6 ML	0.25 g	0.21 g	15.0 s
Friuli	11/09/1976	5.2 Mw	0.16 g	0.20 g	9.5 s

The horizontal components of the accelerograms (in EW and NS directions) have been scaled and modified to match the code elastic spectrum. To assess the compatibility of the accelerograms, the horizontal components have been combined with SRSS technique and compared with the code elastic spectrum multiplied by $\sqrt{2}$. Moreover, the Italian code requires that the mean of the seven elastic SRSS spectrum has to be within the range -10% / +30% of the target elastic spectrum, as shown in Fig.9.

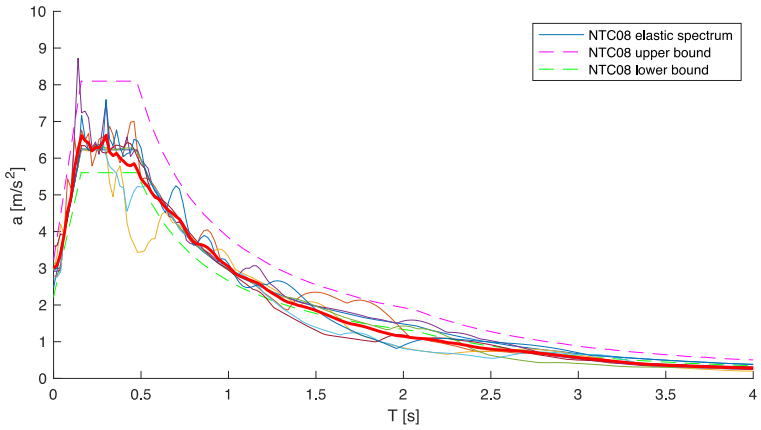

Fig. 9 – Spectrum-compatibility with matched recordings

5. Nonlinear dynamic analyses

An equivalent viscous damping of 1%, proportional to the initial stiffness, was considered in these analyses, carried out using the Hilber-Hughes-Taylor numerical integration algorithm, with an integration time of 0.01 s (that is the same time discretization of the records).

Since the analyses showed only shear mechanisms to be of a critical nature in the seismic assessment of the bridge, their assessment is discussed in this section.

5.1 Verification of fragile mechanisms using the Italian seismic design code

In the shear verification the demand (shear force) is given directly by the analysis, whilst the capacity (shear resistance) is calculated here using the formulae prescribed by the Italian seismic assessment code (NTC18).

The shear capacity of the elements that constitute the Antenna and the Pier has been computed by means of the prescriptions in clause C8.8.5.5 of the NTC18.

$$V_u = V_c + V_N + V_S \tag{1}$$

$$V_C = 0.8 A_C k \sqrt{f_c} \tag{2}$$

$$V_N = N\frac{h-x}{2L_s} \quad (3)$$

$$V_S = \frac{A_{sw}}{s} f_y z \quad (4)$$

The ultimate shear resistance (1) is the sum of the concrete component (2), the axial stress component (3) and the stirrups component (4). It depends on values that change during the time-history analysis, such as the axial force N, the neutral axis position x, and the shear span Ls. For this reason, the ratio between demand and capacity ρ_s has to be evaluated at every instant of the analysis, after which the maximum can be selected, for every analysis and, finally, the mean of the maximum values coming from each of the seven analyses can be obtained. Also, the ultimate shear resistance is a function of the concrete strength f_c and the steel yielding strength f_y, computed as shown in equation (5) and (6).

$$f_c = \frac{f_{cm}}{FC*\gamma_c} \quad (5)$$

$$f_y = \frac{f_{ym}}{FC*\gamma_s} \quad (6)$$

For fragile mechanisms checks, the mean resistances f_{cm} and f_{ym} have to be divided by a confidence factor FC, chosen as a function of structural knowledge level, as well as considering the partial safety factors γc and γs. In Table 9 the material parameters used for this shear checks are given.

Table 9 – Material parameters

Material	**f_{cm}**	**FC**	**γ_c**	**f_c**
Concrete 350/730	42.3 MPa	1.2	1.5	23.5 MPa
Material	**f_{ym}**	**FC**	**γ_c**	**f_y**
Steel Aq50	370.9 MPa	1.2	1.15	268.8 MPa

Further, for collapse limit state fragile mechanisms verifications, the ultimate shear resistance has to be divided by a safety factor γ_{el} = 1.25.

As shown in Fig. 10, a non-negligible number of elements are not verified against shear failure. In Table 10, the values of the shear demand-capacity ratio ρ_s are given, as obtained with both SeismoStruct and Midas Civil; values obtained with the latter are slightly higher probably due to a different status of internal action generated by the Construction Stage Analysis implemented in Midas Civil (see Orgnoni [9]).

Table 10 –Shear demand-capacity ratios of non-verified elements

Element	**SeismoStruct**		**Midas Civil**	
	Section i	Section j	Section i	Section j
PTS_1	**1.41**	**1.42**	**1.58**	**1.52**
PTS_2	0.93	0.98	**1.12**	**1.12**
PTS_3	**1.47**	**1.51**	**1.51**	**1.57**
S_5	**1.13**	**1.16**	**1.41**	**1.52**
ATT	**1.33**	**1.43**	**1.42**	**1.43**
ATS	**1.08**	**1.11**	**1.02**	**1.01**
ALS	0.91	0.93	**1.01**	**1.03**

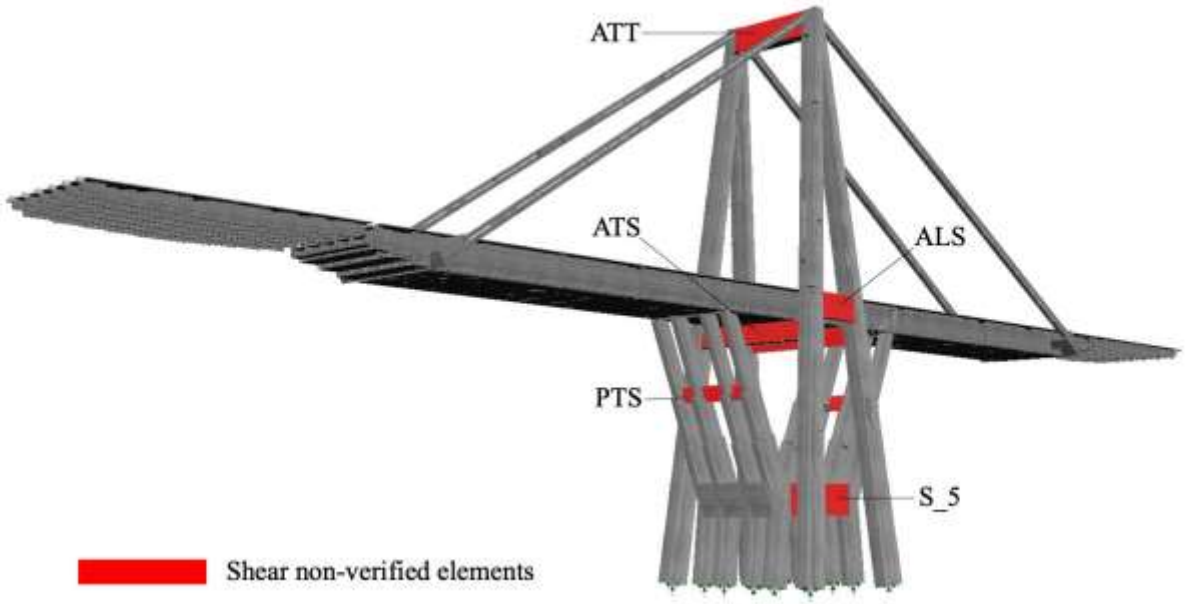

Fig. 10 – Shear non-verified elements

5.2 Verification of fragile mechanisms using MFCT

As discussed in clause C8.8.5.5 of the Italian seismic code, the ultimate shear resistance can be evaluated also through alternative validated models. For this reason, and for the non-verified elements indicated above, the shear strength was also evaluated with the software Response-2000 [13], which makes use of the Modified Compression Field Theory [14].

As shown in Fig. 11 and Table 11, the capacity computed with the Modified Field Compression Theory is higher that the capacity calculated with the empiric formulae suggested by NTC18. Thanks to this increment in shear resistance now all the elements are verified, with the most critical element being the Antenna's top transverse beam (ATT) with a shear demand-capacity ratio of about ρ_s=0.9.

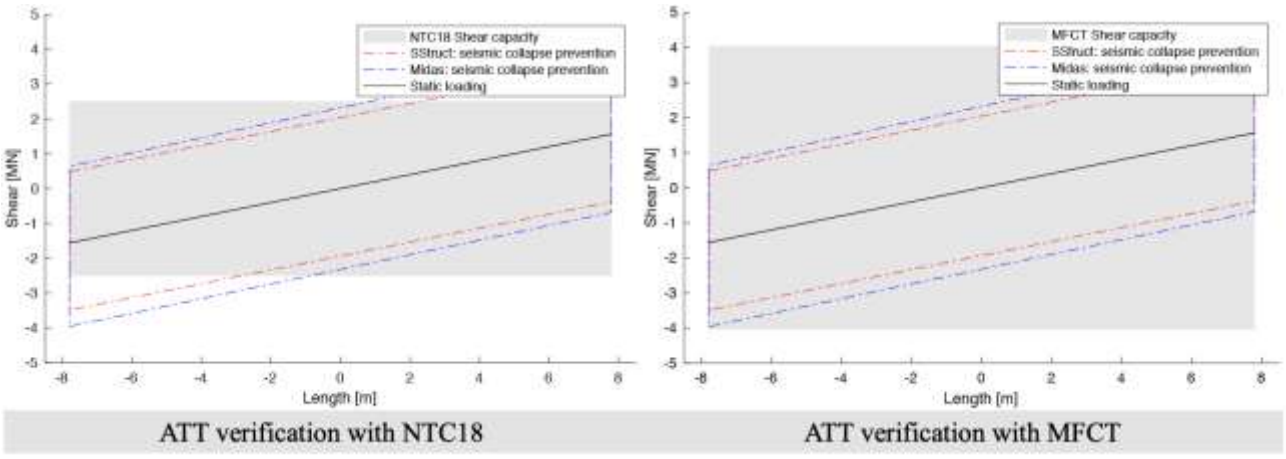

Fig. 11 – Comparison between NTC18 equation and MFCT shear capacity

Table 11 – Comparison between NTC18 equation and MFCT shear capacity

Element	Vu NTC18	Vu MFCT	Increment
PTS_S1	1877 kN	4683 kN	+150%
PTS_S2	1371 kN	1709 kN	+25%
PTS_S3	1877 kN	4683 kN	+150%
SA_5	2614 kN	4762 kN	+82%
ATT	2515 kN	4045 kN	+61%
ATS	1696 kN	2354 kN	+39%
ALS	1976 kN	3260 kN	+65%

5.3 Consequences of a potential local shear failure

Since the previous analyses highlighted a potential criticality in the shear response of the Antenna's top transversal beam, the consequences of a potential failure of such member are herein investigated. Nonlinear dynamic analysis runs featuring progressive modelling collapse capabilities were thus ran, leading to the results reported in Fig. 12.

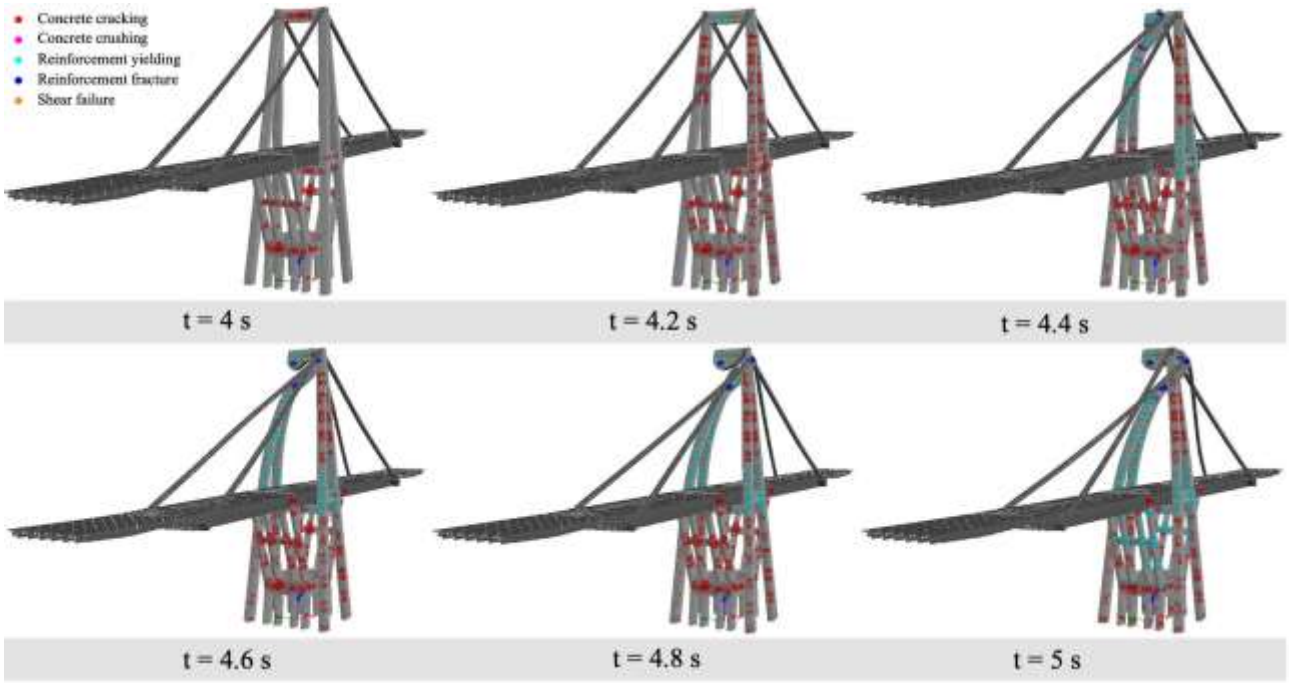

Fig. 12 – Possible collapse scenario triggered by shear failure

6. Conclusions

The study undertaken seemed to indicate a potential criticality in the seismic response of concrete balanced-system bridge structures. This is not necessary a result of an overlook by the designers of the bridges, but rather more a consequence of the fact that in 60s, when these bridges were constructed, design codes did not necessarily feature robust seismic design prescriptions.

As discussed in the Introduction, in addition to the case-study bridge (Polcevera Viaduct, collapsed on August 14, 2018), there are other similar bridges/viaducts in the World, all built in the same period, and exposed to levels of seismic hazard that are at least equal, if not higher, then the one considered for the case-study discussed in this paper (PGA = 0.18g). Given that the type of member failure identified as critical (i.e. shear failure of the Antenna's top transversal beam) has been shown to then lead to the complete collapse of the bridge, a thorough seismic assessment of such bridges is probably warranted.

Acknowledgements

The authors would like to acknowledge Martina Caruso for the precious assistance in the selection and scaling of the records employed in the nonlinear dynamic analyses.

References

[1] Morandi R. (1967): Il viadotto sul Polcevera per l'autostrada Genova-Savona. *L'Industria Italiana del Cemento*, XXXVII, 849-872.

[2] Calvi G.M., Moratti M., O'Reilly G.J., Scattarreggia N., Monteiro R., Malomo D., Calvi P.M., Pinho R. (2019): Once upon a time in Italy: The tale of the Morandi bridge. *Structural Engineering International*, 29(2): 198-217.

[3] Seismosoft (2018). SeismoStruct – A computer program for static and dynamic nonlinear analysis of framed structures, *http://www.seismosoft.com*

[4] Seismosoft (2018). SeismoStruct Verification Report, *http://www.seismosoft.com*

[5] Mander, J.B., Priestley M.J.N., and Park R. (1988): Theoretical stress-strain model for confined concrete. *Journal of Structural Engineering*, 114.8:1804-1826.

[6] Menegotto, M., and Pinto, P. (1973): Method of analysis for cyclically loaded RC plane frames including changes in geometry and non-elastic behavior of elements under combined normal force and bending. In *Proceedings of the IABSE Symposium on resistance and ultimate deformability of structures acted on by well defined repeated loads*, Zurich, Switzerland, 15–22.

[7] Verderame G. M., Ricci P., Esposito M., and Sansiviero F.C. (2011): Le caratteristiche meccaniche degli acciai impiegati nelle strutture in CA realizzate dal 1950 al 1980. *Atti del XXVI Convegno Nazionale AICAP - le prospettive di sviluppo delle opere in calcestruzzo strutturale nel terzo millennio* [in Italian], 19-21.

[8] On-line Midas Civil manual, *http://manual.midasuser.com*

[9] Orgnoni A. (2019): Critical review and modelling of the construction sequence of the Polcevera Viaduct. *MEng Dissertation, Department of Civil Engineering and Architecture, University of Pavia, Pavia, Italy.*

[10] Ministero Infrastrutture e Trasporti (2018), Aggiornamento Norme tecniche per le Costruzioni, G.U. 20/02/2018, Suppl. Ord n. 8 (NTC 2018).

[11] Consiglio Superiore dei Lavori Pubblici (2019) Istruzioni per l'applicazione dell'"Aggiornamento delle Norme tecniche per le costruzioni", G.U. Serie Generale del 11-02-2019, n.35 - Suppl. Ordinario n. 5.

[12] Seismosoft (2018). SeismoSelect, *http://www.seismosoft.com*

[13] Bentz E. C. (2017): Response-2000, *http://www.ecf.utoronto.ca/~bentz/r2k.htm*

[14] Vecchio F.J., Collins M.P. (1986): The modified compression field theory for reinforced concrete elements subjected to shear. *ACI Journal*, 1986; 83(2):219–231.